for correcting for the change in charge distribution, and the present approach represents the most accurate method of obtaining an estimate of $E°_{(5)}$. The resulting values of $E°_{(5)}$ were −1.19, −1.73, −1.05, and −0.94 V for methylamine, ethylamine, dimethylamine, and trimethylamine, respectively. Likewise, utilizing the values of $\Delta G°_{(3)}$ derived above, one can estimate that $E°_{(1)}$ has values of about −1.5, −1.9, −1.5, and −1.4 V for the same amines, respectively. The large negative values of $E°_{(1)}$ confirm the strong reductive power of these $R^1R^2NCR^3H^•$ radicals. Previous estimates of $E°_{(1)}$ in aqueous solution have been in the region of −1.0 V.[40] Equilibrium measurements of these quantities in water will be very difficult because of the transitory nature of both the radicals and the iminium products. Thus, this is a case where theoretical investigations of the solution free energies of the iminium species would be of considerable interest, since they have the potential to reduce the uncertainties in the calculation of $E°_{(1)}$.

5. Summary

In the present work, thermochemical functions for aminoalkyl and alkylaminium free radicals and related species were derived by combining results from high-level ab initio calculations with known experimental data. In calculating $\Delta G°$(soln) for the neutral radicals from eq 8, the solution free energies are partitioned as the sum of hydrogen-bonding ($\Delta G°$(HB)) and non-hydrogen-bonding ($\Delta G°$(NHB)) terms, and the latter is treated as a constant which depends on the number of CH_2 units in the molecule. It was argued that the difference in $\Delta G°$(soln) between α-carbon radicals, $R^1R^2NCR^3H^•$, and the parent molecules, $R^1R^2NCR^3H_2$, is less than 2 kJ mol^{-1} and can be neglected. For the charged species, the difference between trimethylaminium ($(CH_3)_3N^{•+}$) and trimethylammonium ($(CH_3)_3NH^+$) could be derived from experimental estimates of $\Delta G°$(soln) of the two species. The increase in magnitude of the solution free energy of $(CH_3)_3N^{•+}$ over that of $(CH_3)_3NH^+$ by 30 kJ mol^{-1} is assumed to apply in general to the $R^1R^2NCR^3H_2^{•+}$ species and is used to derive heats of solution for the radical cations of methylamine, ethylamine, and dimethylamine. On the basis of the above analysis, the calculated values of $E°_{(6)}$ for reaction 6 and $E°_{(1)}$ for reaction 1 were very reasonable. The results confirmed the strong reducing character of the α-amino radicals.

Acknowledgment. The financial support of the Natural Sciences and Engineering Research Council of Canada is gratefully acknowledged.

Supplementary Material Available: MP2/6-31+G* optimized structures for $H_2NCH_2^+$, $H_2NCH_2^•$, H_2NCH_3, $H_2NCH_3^{•+}$, $H_3NCH_2^{•+}$, $(CH_3)_2NCH_2^+$, $(CH_3)_2NCH_2^•$, $(CH_3)_3N$, and $(CH_3)_3N^{•+}$ (Table S-I), HF/6-31G* frequencies and infrared intensities for the above molecules (Table S-II), and ideal gas thermodynamic properties (Table S-III) (4 pages). Ordering information is given on any current masthead page.

(40) (a) Adrieun, P. A.; Saveant, J. M. *Bull. Soc. Chim. Fr.* **1968**, 4671. (b) Monserrat, K.; Foreman, T. K.; Grätzel, M.; Whitten, D. G. *J. Am. Chem. Soc.* **1981**, *103*, 6667. (c) Hiller, K. O.; Asmus, K. D. *J. Phys. Chem.* **1983**, *87*, 3682.
(41) Lossing, F. P.; Lam, Y. T.; Maccoll, A. *Can. J. Chem.* **1981**, *59*, 2228.
(42) Klots, C. E. *J. Phys. Chem.* **1981**, *85*, 3585. Parsons, R. *Standard Potentials in Aqueous Solution*; Bard, A. J., Parsons, R., Jordan, J., Eds.; IUPAC Commissions on Electrochemistry and Electroanalytical Chemistry; M. Dekker: New York, 1985; p 13.
(43) Lim, C.; Bashford, D.; Karplus, M. *J. Phys. Chem.* **1991**, *95*, 5610.

An MC-SCF Study of the S_1 and S_2 Photochemical Reactions of Benzene

Ian J. Palmer,[†] Ioannis N. Ragazos,[†] Fernando Bernardi,*[,‡] Massimo Olivucci,[‡] and Michael A. Robb*[,†]

Contribution from the Dipartimento di Chimica "G.Ciamician" dell'Universita di Bologna, Via Selmi 2, 40126 Bologna, Italy, and the Department of Chemistry, King's College London, Strand, London WC2R 2LS, U.K. *Received July 16, 1992*

Abstract: An MC-SCF/4-31G characterization of the possible photochemical pathways of S_1 and S_2 benzene is documented. A complete mechanistic scheme is presented through the characterization of minima and transition states on S_0, S_1, and S_2. The full characterization of Born–Oppenheimer violation regions, where the products of the diabatic processes relax to lower electronic states, is also performed. On the S_0 surface the reversion of Dewar benzene to benzene is shown to occur via a concerted path along a symmetric coordinate where the bridgehead Dewar benzene bond and the pair of "quinoid" double bonds are being synchronously broken. No evidence for an asymmetric path could be found. The ground-state potential energy surface along the reaction path between benzene and benzvalene has a flat diradicaloid region corresponding to prefulvene. However, prefulvene itself is a transition state. The S_1 reaction path from benzene toward prefulvene contains an excited-state minimum with D_{6h} symmetry and a transition state between this minimum and a prefulvene diradicaloid located on the ground-state surface. The Born–Oppenheimer violation region has been fully characterized by optimizing the conical intersection that occurs between the transition state on S_1 and the prefulvene biradicaloid region on S_0. The existence of a low-energy diradicaloid minimum on S_2 with an immediately adjacent S_1/S_2 conical intersection at only slightly higher energy has been demonstrated. This suggests that the radiationless decay from S_2 is almost completely efficient in contrast to the commonly held view. The different photochemistry of S_2 is shown to arise from the fact that the S_0/S_1 decay that occurs subsequent to passage through the S_1/S_2 conical intersection occurs at a geometry on the S_0/S_1 crossing surface where there is a C_1–C_4 bond similar in length to the bridgehead bond of the S_0 transition state between Dewar benzene and benzene. Thus there exists a ground-state reaction path to Dewar benzene from a high-energy region of the S_0/S_1 crossing surface.

Introduction

Photoexcitation of benzene permits the demise of the planar aromatic hexagonal ring system and movement along reaction coordinates toward the highly strained nonaromatic multiring valence isomers of benzene. The five observed valence isomers of benzene (Chart I) are the familiar Kekule form (**1**), Dewar benzene (**2**), benzvalene (**3**) (Huckel benzene), prismane (**4**) (Ladenburg benzene), and the bicyclopropenyl structure (**5**); all

Chart I

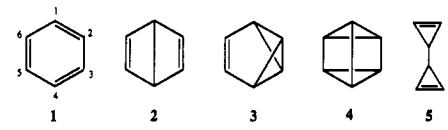

[†] King's College London.
[‡] Universita di Bologna.

0002-7863/93/1515-673$04.00/0

Scheme I

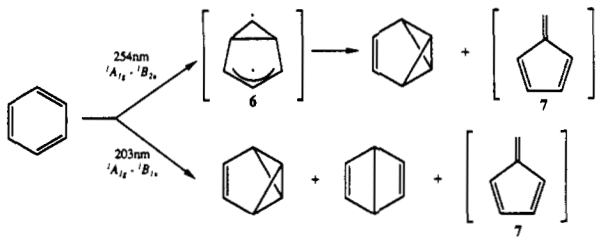

may be represented by the general formula $(CH)_6$.

There is, apparently, no direct path from benzene to prismane or the bicyclopropenyl structure. However, it has been shown experimentally that **2** and **4** interconvert in what may be viewed as essentially an intramolecular [2 + 2] cycloaddition of the two ethylenic fragments of Dewar benzene.[1] In a recent theoretical study of this process, we have demonstrated the existence of a Born–Oppenheimer violation[2] region along the highly strained nonadiabatic photochemical reaction coordinate connecting these valence isomers.[3] Although no bicyclopropenyl is observed from the photoreactions of benzene, the conversion of **5** to **1** is achieved photochemically. Thus the photochemistry of S_1 and S_2 benzene involves the production of benzvalene and Dewar benzene, and a mechanistic rationalization of these processes is the subject of this paper.

These S_1 and S_2 reactions are nonadiabatic. The reaction starts on an excited-state potential surface and proceeds directly to a bonding ground-state configuration via a Born–Oppenheimer violation. For most photoreactions, it is still largely unknown at what point along the reaction coordinate the products of the diabatic processes relax to the electronic ground state. This point of relaxation may be before or after the transition state. Thus the characterization of a photochemical reaction involves, in addition to the usual study of ground- and excited-state reaction paths, a characterization of the region where Born–Oppenheimer violation occurs and the system decays nonradiatively to the ground state. The photochemistry of benzene is almost unique. The efficiency of internal conversion from upper electronic states to S_1 (which is normally 100% for organic molecules in dilute solution) is apparently less than 100% for benzene, and one observes a distinct photochemistry from S_2. Recently we have implemented the theoretical methodology[4] for studying the Born–Oppenheimer violation region of the excited-state surface with the same level of accuracy that can be used to study ground-state reaction paths. In this paper, this methodology is applied to the characterization of such regions in the S_1 and S_2 reactions of benzene.

The singlet photochemistry of benzene is summarized in Scheme I. The valence isomerization reactions of benzene from its lower excited states have been extensively studied from an experimental point of view, and theoretical models have been proposed to offer explanations for the empirical observations (for a general discussion, see ref 2, 5, and 6). When benzene is irradiated with a 254-nm source, the first excited singlet state ($^1B_{2u}$) is populated and benzvalene and fulvene are observed as the products of a nonadiabatic process.[7-10] Fulvene (7), which is an isomer though not a *valence* isomer of benzene, is assumed to be formed via secondary isomerization of the benzvalene. It is now generally accepted that the reaction path originating in S_1 benzene passes through the ground-state intermediate prefulvene (Scheme I, **6**), which is a possible precursor to benzvalene and fulvene. The quantum yield of benzvalene increases with decreasing wavelength, and this observation was assumed to indicate a barrier on the excited-state surface before the Born–Oppenheimer violation region where nonradiative decay to the ground state may occur. However, there is an important photophysical effect that was first reported in 1968[8] that relates to this photochemical reaction: all observed fluorescence from the S_1 benzene excited state vanishes with a vibrational excess of ca. 3000 cm^{-1}. It was suggested that the sudden loss of fluorescence could not be explained by conventional nonradiative decay mechanisms, e.g., internal conversion (IC), intramolecular vibrational relaxation (IVR), etc., and hence many possible mechanisms have been proposed for the mysterious decay route, termed "channel 3". There is a large literature on the subject; see, for example, refs 11–13 and references therein for experimental aspects and references 14–18 for theoretical examples in which attempts have been made to model the dynamics of channel 3 decay. However, most dynamics calculations are model computations in which real potential energy surface data has not been included and only one or two nuclear modes have been considered. The most comprehensive dynamics study is due to Kato,[19] who has used an ab initio potential along an out-of-plane distortion corresponding to a prefulvenic coordinate. Remarkably, there seems to have been no study in which all the nuclear degrees of freedom are included. Finally, a very recent experimental study on rotationally resolved fluorescence excitation and resonance-enhanced multiphoton ionization spectra of vibrational bands near the channel 3 threshold has cast doubt on the involvement of a new nonradiative decay mechanism in the photophysics of this state at all.[11]

The second excited singlet state of benzene ($^1B_{1u}$) is populated via excitation with a source of 203 nm,[20] and three products result—Dewar benzene, fulvene, and benzvalene in a ratio of 1:2:5. Once again, fulvene is assumed to result from secondary isomerization of the benzvalene produced.

Experimental evidence appears to point to little involvement of the triplet manifold in these valence isomerization processes. However, both benzvalene and Dewar benzene appear to be very susceptible to triplet-sensitized adiabatic rearomatization, which results in a destructive quantum chain reaction.[1,21] Since the only involvement of the triplet in these reactions is apparently detrimental, it has been observed that the addition of triplet quenchers or energy acceptors increases yields of benzvalene and Dewar benzene from these reactions.[10,20]

The important role that benzene has played in the development of organic chemistry, coupled with its unique aromatic nature and highly symmetric structure, has made it a popular target for theoretical study. The majority of studies related to the excited states of benzene have been concerned with the computation of photophysical phenomenon (see, for example, refs 22 and 23 and references therein). The recent work of Roos et al.[23] provides a definitive study of the vertical excitations of benzene. They have

(1) Turro, N. J.; Ramamurthy, V.; Katz, T. J. *Nouv. J. Chim.* **1977**, *1*, 363–365.
(2) Bryce-Smith, D.; Gilbert, A. *Tetrahedron* **1976**, *32*, 1309–1326.
(3) Palmer, I. J.; Robb, M. A.; Ollivucci, M.; Bernardi, F. *J. Org. Chem.* **1992**, *57*, 5081–5087.
(4) Ragazos, I. N.; Robb, M. A.; Olivucci, M.; Bernardi, F. *Chem. Phys. Lett.* **1992**, *197*, 217–223.
(5) Bryce-Smith, D.; Gilbert, A. In *Rearrangements in Ground and Excited States*; de Mayo, P., Ed.; Academic Press: London, 1980; Vol. 3, pp 349–379.
(6) Scott, L. T.; Jones, M., Jr. *Chem. Rev.* **1972**, *72*, 181–202.
(7) Wilzbach, K. E.; Ritscher, J. S.; Kaplan, L. *J. Am. Chem. Soc.* **1967**, *89*, 1031–1032.
(8) Kaplan, L.; Wilzbach, K. E. *J. Am. Chem. Soc.* **1968**, *90*, 3291–3292.
(9) Wilzbach, K. E.; Harhness, A. L.; Kaplan, L. *J. Am. Chem. Soc.* **1968**, *90*, 1116–1118.
(10) Lee, S. A.; White, J. M.; Noyes, W. A. *J. Chem. Phys.* **1976**, *65*, 2805–2811.
(11) Riedle, E.; Weber, T.; Shubert, U.; Neusser, H. J.; Schlag, E. W. *J. Chem. Phys.* **1990**, *93*, 967–978.
(12) Suzuki, T.; Ito, M. *J. Chem. Phys.* **1989**, *91*, 4564–4570.
(13) Riedle, E.; Neusser, H. J.; Schlag, E. W. *Philos. Trans. R. Soc. London A* **1990**, *332*, 189–201.
(14) Hornburger, H.; Sharp, C. M. *Chem. Phys.* **1986**, *101*, 67–79.
(15) Sobolewski, A. L.; Czerminski, R. *Chem. Phys.* **1989**, *130*, 123–128.
(16) Sobolewski, A. L. *J. Chem. Phys.* **1990**, *93*, 6433–6439.
(17) Sobolewski, A. L.; Lim, E. C.; Siebtand, W. *Int. J. Quantum Chem.* **1991**, *39*, 309–324.
(18) Sobolewski, A. L.; Domke, W. *Chem. Phys. Lett.* **1991**, *180*, 381–386.
(19) Kato, S. *J. Chem. Phys.* **1988**, *88*, 3045–3056.
(20) Bryce-Smith, D.; Gilbert, A.; Robinson, D. A. *Angew. Chem., Int. Ed. Engl.* **1971**, *10*, 745–746.
(21) Renner, C. A.; Katz, T. J.; Pouliquen, J.; Turro, N. J.; Waddell, W. H. *J. Am. Chem. Soc.* **1975**, *97*, 2568–2570.
(22) Kitao, O.; Nakatsuji, H. *J. Chem. Phys.* **1987**, *87*, 1169–1182.
(23) (a) Matos, J. M. O.; Roos, B. O.; Malmqvist, P. *J. Chem. Phys.* **1987**, *86*, 1458–1466. (b) Roos, B. O.; Andersson, K.; Fulscher, M. P. *Chem. Phys. Lett.* **1992**, *192*, 5–13.

shown that the excited states of benzene can be classified into two types, covalent (A $^1B_{2u}$ D $^1E_{2g}$) and ionic/Rydberg (B $^1B_{1u}$ C $^1E_{1u}$), where we use the usual X A B C, etc., to denote the ordering of the states. A satisfactory description of the covalent states may be obtained with "normal" p^π molecular orbitals, but in order to characterize the ionic/Rydberg states of benzene, diffuse p^π orbitals are required. It appears that the ionic states are very sensitive to the basis set used, but the covalent states are not. However, the states that are of photochemical interest are the covalent states, which are easily discussed in a VB formalism. The X state is obviously the sum of the two Kekule VB structures, while the A $^1B_{2u}$ may be viewed as the "anti-Kekule" combination. The D $^1E_{2g}$ states are combinations of the Dewar structures. The S_1 state is covalent (as is evident in the theoretical computations and experimentally, where absorption is of low intensity). The S_2 state is B $^1B_{1u}$ in the vertical excitation region; however, this has been shown to cross[24] with the states originating from D $^1E_{2g}$ along a reaction coordinate leading to Dewar benzene. Thus the S_2 state that yields the photochemistry is undoubtedly a covalent state that has its origins in the covalent D $^1E_{2g}$ state.

There have been only a few theoretical studies[19,24-26] concerned with the photochemical interconversion of benzene and its valence isomers. Only a single study has been reported for the S_2 surface. Using SCF-CI, Meisl and Janoschek[24] found a diradicaloid minimum on the surface that correlates with the vertically excited D $^1E_{2g}$ state. At this geometry, this state lies below that which correlates with the vertically excited B $^1B_{1u}$ state. However, no attempt was made to characterize a Born–Oppenheimer violation region. In contrast, the reactions from S_1 benzene have received most of the theoretical attention.[19,25] The majority of studies have used a "coordinate driven" approach along an assumed reaction coordinate between benzene and prefulvene (**6**). The most detailed study is due to Kato.[19] He studied the ground state and lowest singlet excited state of benzene along a coordinate connecting benzene and prefulvene (**6**). The reaction path was explored using a coordinate driven technique corresponding to the formation of the C_2–C_6 bond in **6** (for a discussion of the limitations of such a method, see ref 27). He has located an approximate transition structure on S_1 and an S_1/S_0 crossing. Based upon a sixth-order polynomial representation of the surface along this path, he has performed dynamics computations related to the internal conversion to the ground state via both "surface hop" and tunnelling mechanisms.

Our aim in this paper is to present a unified mechanism that rationalizes both the S_1 and S_2 photochemistry of benzene. In order to accomplish this, we need to characterize, with full geometry optimization within the MC-SCF approach, not only the photochemical reaction paths on the two lowest energy covalent excited states of benzene (that originate as A $^1B_{2u}$ and D $^1E_{2g}$ in the Franck–Condon region) but also, with equal accuracy, the Born–Oppenheimer violation region where the products of the excited-state processes relax to the electronic ground state. In addition, since there remains the question of whether the transition structure occurs before or after the Born–Oppenheimer violation region, one must also characterize the ground-state reaction paths. In addition to providing a rationalization of the photochemistry, the nature of the S_1 and S_2 together with the characterization of the Born–Oppenheimer violation region should suggest improved models for studying the dynamics of the channel 3 decay process.

Methodological and Computational Details

While the location of minima and transition states is readily accomplished using standard methods, the characterization of the Born–Oppenheimer violation region where decay occurs from the excited-state surface to the ground-state surface is not so straightforward, and we now give some discussion of the point. Various models for the surface crossing region have been discussed in refs 28–32. The probability of radiationless decay is given as

$$P = \exp[-(\pi/4)\zeta] \tag{1}$$

where ζ is the Massey parameter, given as

$$\zeta = \frac{\Delta E(\mathbf{q})}{\frac{\hbar}{2\pi}|\dot{\mathbf{q}}||g(\mathbf{q})|} \tag{2}$$

where $\mathbf{q}$ is a vector of nuclear displacement coordinates. The term $g(\mathbf{q})$ is the nonadiabatic coupling matrix element defined as

$$g(\mathbf{q}) = \langle\psi_1|\partial\psi_2/\partial\mathbf{q}\rangle \tag{3}$$

while $|\dot{\mathbf{q}}|$ is the magnitude of the velocity along the reaction path and ΔE is the energy gap. As we approach a point where the surfaces cross, the decay probability becomes 1. Further, unless ΔE is less than about 2 kcal mol^{-1}, the decay probability is vanishingly small. Thus the decay must occur in regions where a crossing occurs. The crossing region of two potential energy surfaces is characterized by the following statement: *Two surfaces, even with the same symmetry, intersect in an* $(n-2)$*-dimensional hyperline (the crossing surface) as the energy is plotted against the n nuclear coordinates.* This statement defines a topological feature called a conical intersection[33-36] (see, for example, the discussion in the book of Salem[32]). Dynamics computations indicate that decay via a conical intersection occurs within a single vibrational period.[37] At a conical intersection, one can distinguish two directions, say $\mathbf{x}_1$ and $\mathbf{x}_2$, such that if one were to plot the energy in the subspace of these two geometric variables (combinations of the bond lengths, angles, etc.), the potential energy would have the form of a double cone in the region of the degeneracy. The remaining $n-2$ directions define the crossing surface over which the energies of ground and excited states are equal. Movement in the plane $(\mathbf{x}_1\mathbf{x}_2)$ from a point on the intersection will result in the degeneracy being lifted. The two vectors $\mathbf{x}_1$ and $\mathbf{x}_2$ correspond to the direction of the gradient difference vector $\mathbf{x}_1 = \partial(E_2 - E_1)/\partial\mathbf{q}$, where $\mathbf{q}$ is a nuclear displacement vector, and to the direction of the nonadiabatic coupling vector $\mathbf{x}_2$, defined in eq 3. The gradient difference vector "points" to the "bottom" of the cone, and the nonadiabatic coupling vector is approximately at 90°.

Thus the Born–Oppenheimer violation region can be determined and characterized in much the same way as a transition state. We are interested in the lowest energy point on the $(n-2)$-dimensional hyperline which corresponds to a well-defined geometry of the system. In the optimization, the energy is minimized in the $n-2$ variables of the subspace orthogonal to $\mathbf{x}_1$ and $\mathbf{x}_2$ (i.e., the vectors $\mathbf{x}_1$ and $\mathbf{x}_2$ are the directions of the constraints imposed during the optimization). The gradient on the excited-state potential energy surface will not be 0 at a conical interesection point, since it "looks like" the vertex of an inverted cone. The gradient is only 0 in the $n-2$ dimensional space orthogonal to $\mathbf{x}_1$ and $\mathbf{x}_2$. This situation is distinguished from an "avoided crossing minimum" of two surfaces where the gradient on the excited-state potential energy surface would go to 0 in the full space of geometrical variables. The actual algorithm used in the optimization is documented elsewhere.[4]

All calculations have been performed with the implementation of the MC-SCF procedure available in the Gaussian 91 package.[38] The choice of active space is unambiguous and is comprised of the six electrons and orbitals which form the π system of benzene. The 175-term, 6-orbital MC-SCF wave function that results is capable of describing all the states that can arise from all possible arrangements of six electrons in six orbitals. *All the orbitals are fully utilized and optimized* in the com-

(24) Meisl, M.; Janoschek, R. *J. Chem. Soc., Chem. Commun.* **1986**, 1066–1067.
(25) Oikawa, S.; Tsunda, M.; Okamura, Y.; Urabe, T. *J. Am. Chem. Soc.* **1984**, *106*, 6751–6755.
(26) Tsunda, M.; Oikawa, S.; Kimura, K. *Int. J. Quantum Chem.* **1980**, *18*, 157–164.
(27) Schlegel, H. B. *Adv. Chem. Phys.* **1987**, *67*, 249–286.
(28) Van der Lugt, W. T. A. M.; Oosteroff, L. J. *J. Am. Chem. Soc.* **1969**, *91*, 6042.
(29) Gimbert, D.; Segal, G.; Devaquet, A. *J. Am. Chem. Soc.* **1975**, *97*, 6629.
(30) Michl, J.; Bonacic-Koutecky, V. *Electronic Aspects of Organic Photochemistry*; Wiley: New York, 1990.
(31) Bonacic-Koutecky, V.; Koutecky, J.; Michl, J. *Agnew. Chem., Int. Ed. Engl.* **1987**, *26*, 170–189.
(32) Salem, L. *Electrons in Chemical Reactions: First Principles*; Wiley: New York, 1982.
(33) Von Neunann, J.; Wigner, E. *Physik. Z.* **1929**, *30*, 467.
(34) Teller, E. *J. Phys. Chem.* **1937**, *41*, 109.
(35) Herzberg, G.; Longuet-Higgins, H. C. *Trans. Faraday Soc.* **1963**, *35*, 77.
(36) Herzberg, G. *The Electronic Spectra of Polyatomic Molecules*; Van Nostrand: Princeton, 1966; pp 442.
(37) Manthe, U.; Koppel, H. *J. Chem. Phys.* **1990**, *93*, 1669.
(38) *Gaussian 91* (Revision C); Frisch, M. J.; Head-Gordon, M.; Trucks, G. W.; Foresman, J. B.; Schlegel, H. B.; Raghavachari, K.; Robb, M.; Wong, M. W.; Replogle, E. S.; Binkley, J. S.; Gonzalez, C.; Defrees, D. J.; Fox, D. J.; Baker, J.; Martin, R. L.; Stewart, J. J. P.; Pople, J. A. Gaussian, Inc., Pittsburgh, PA, 1991.

Table I. Energies of Optimized Structures on S_0, S_1, and S_2 Potential Energy Surfaces of Benzene

structure	geometry	energy (E_h)	relative energy, kcal mol^{-1}
	S_0 Structures		
D_{6h} benzene	Figure 1a	−230.4543	X
		−230.2695	A($^1B_{2u}$) 5.02 eV
		−230.1511	D($^1E_{2g}$) 8.25 eV
Dewar benzene	Figure 1b	−230.3010	96.2
benzvalene	Figure 1c	−230.2881	104.3
benzene → Dewar benzene TS[a]	Figure 2a	−230.2693	120.1
prefulvene TS	Figure 2b	−230.2544	125.4
perbenzvalene	Figure 2d	−230.2548	125.2
prebenzvalene → benzene TS	Figure 2c	−230.2527	126.5
prebenzvalene → benzvalene TS	Figure 2e	−230.2546	125.3
	S_1 Structures		
stretched D_{6h} benzene	Figure 3a	−230.2774	0.0
stretched D_{6h} benzene → prefulnene TS	Figure 3b	−230.2407	23.0
S_1/S_0 minimum conical intersection	Figure 3c	−230.2368[SA b]	26.0
	S_2 Structures		
quinoid D_{2h} third-order TS	Figure 5a	−230.1823	6.3
quinoid chair TS	Figure 5c	−230.1878	2.9
quinoid boat	Figure 5b	−230.1924	0.0
S_2/S_1 conical intersection	Figure 5c	−230.1799[SA]	9.1
S_1/S_0 conical intersection (adjacent to S_2/S_1)	Figure 8	−230.1698[SA]	14.2

[a] TS = transition state. [b] SA = state averaged orbitals. The energies of these computations are not strictly comparable with the others. Optimization of the higher eigenvalue would lower the energy by approximately 2 kcal mol^{-1}.

putation, but only the active orbitals can have variable occupancy. Thus no assumption of σ/π separability is implied. The identification of six p^π active orbitals is merely a specification of which orbitals can have occupancy other than 2. As the geometry is changed from a planar arrangement, the optimization of the orbitals mixes σ/π orbitals to give the lowest energy. The only type of interaction that is not included explicitly at the CI level would result from single excitations of the σ backbone. However, this type of interaction is included through the Brillouin condition, satisfied by the optimum MC-SCF orbitals.

At this point it is convenient to discuss the limitations on our calculations that arise from the basis set used. Since we have explored the ground-state and two excited-state surfaces as well as the Born–Oppenheimer violation region in considerable detail, we have restricted ourselves to a modest 4-31G basis set. This is adequate for determining the surface topology and optimized geometries of the covalent states (i.e., reproduction of the number and nature of critical points). In order to obtain a description of the ionic states, a basis set containing diffuse functions and an increased active space consisting of both "tight" and "diffuse" p^π orbitals are required.[23] Roos et al.[23] show that while the description of the ionic states is sensitive to basis sets, the number of active orbitals, and electron correlation, the covalent states are well described by a six-active-orbital space. Our calculations, therefore, offer a description of the lowest energy singlet covalent states, which we believe to be of main importance in the chemical processes.

Results and Discussion

A. Ground-State Potential Energy Surface. Other than the minima, the ground-state potential energy surface of the benzene isomers does not seem to have been documented in detail, (although the reaction path from benzene to prefulvene **6** has been partly documented, as noted previously). Thus we begin our discussion of the topological features of this surface as a prelude to the discussion of the photochemistry. The energetic information relating to all of the optimized structures located on ground and excited states is given in Table I. Note that the conical intersection geometries were obtained using state-averaged orbitals (a necessary requirement because of the degeneracy), and thus the energies here are not strictly comparable with the other computations. The energies corresponding to vertical excitation for the covalent A and D states are in good agreement with the much more extensive MC-SCF computations reported in ref 23, which gives an indication that the basis sets used in this work are adequate for describing the covalent excited states.

The 4-31G MC-SCF optimized structures for the ground-state minima of benzene, Dewar benzene, and benzvalene are shown in Figures 1a, 1b, and 1c, respectively. Note that the bridgehead bond in Dewar benzene is considerably stretched at 1.64 Å. Also, there is a slight asymmetry in the benzvalene molecule. (This is an artifact of the MC-SCF active space, since two of the σ bonds

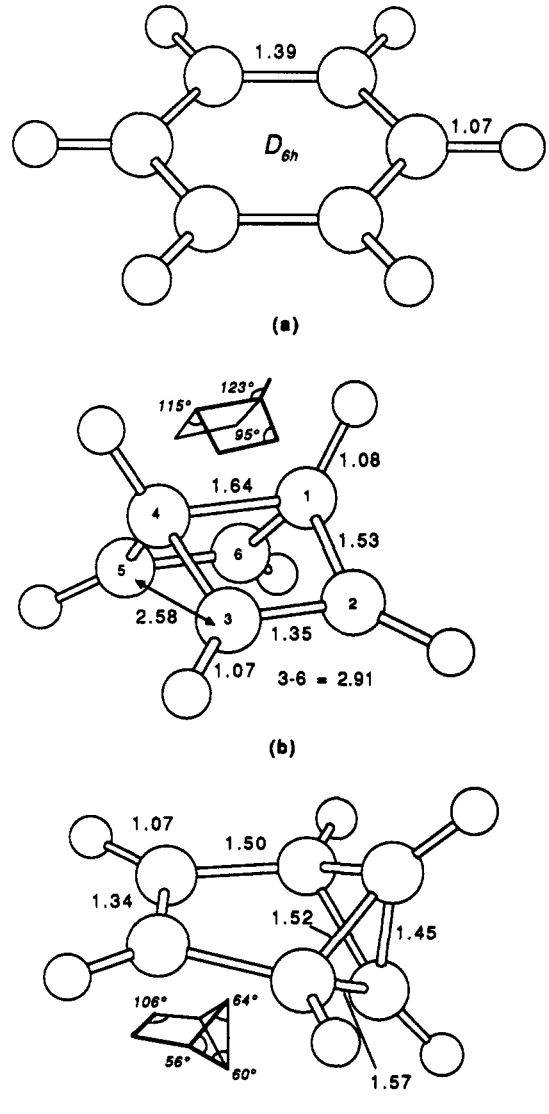

Figure 1. Optimized geometries for S_0 minima for (a) benzene, (b) Dewar benzene, and (c) benzvalene.

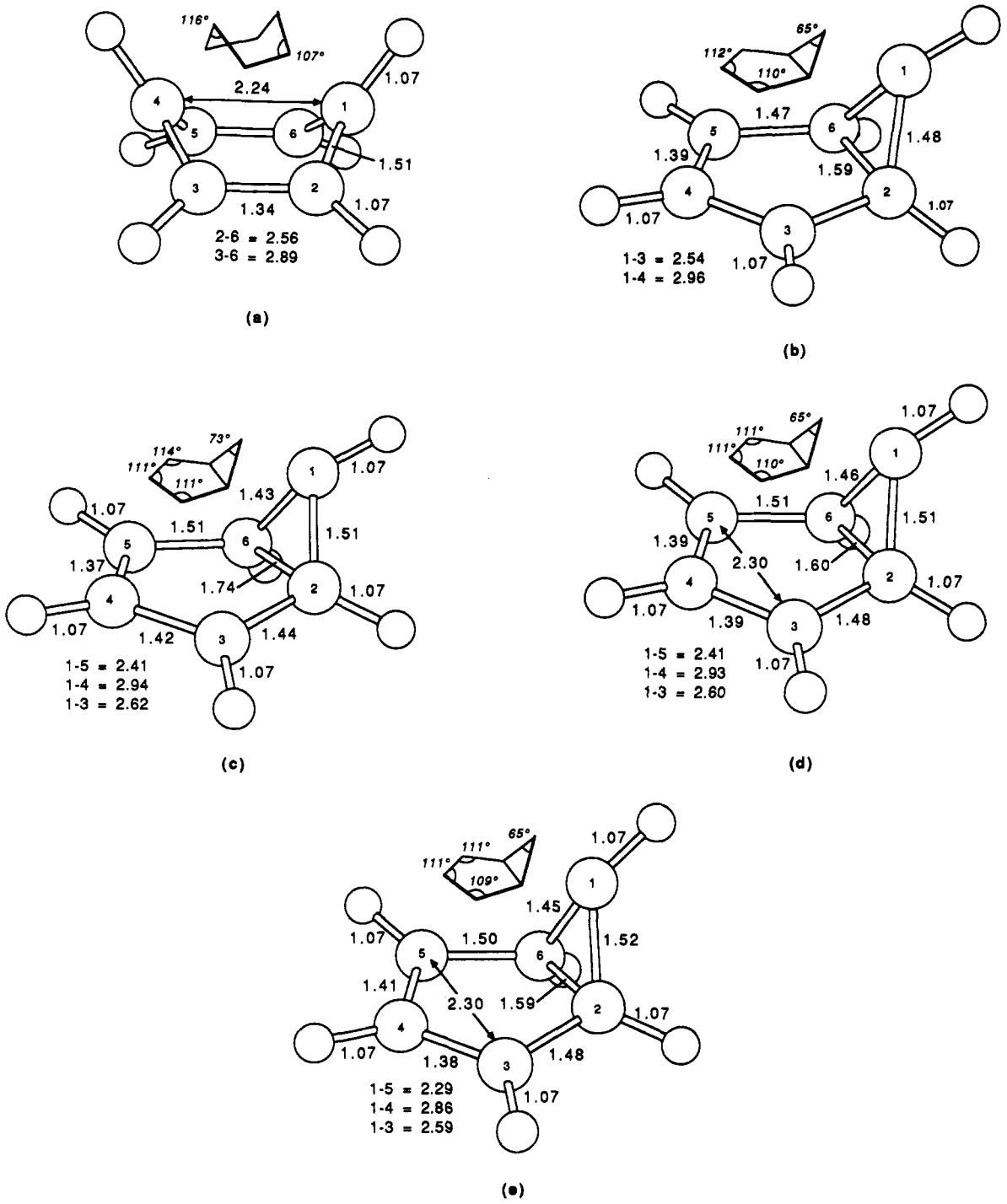

Figure 2. Optimized geometries on S_0 (a) benzene → Dewar benzene transition state, (b) prefulvene (transition state), (c) prebenzvalene → benzene transition state, (d) prebenzvalene (minimum), and (e) prebenzvalene → benzvalene transition state.

of the cyclopropyl fragments are included in the active space and two are not). The computed structural parameters are in acceptable agreement with previous theoretical computations[39,40] and the experimental data cited therein. We now discuss the possible reaction paths connecting these minima.

The reversion of Dewar benzene to benzene could be thought of as a ring opening of a cyclobutene ring fragment in the Dewar benzene molecule, and thus an asymmetric path may be proposed. This path as well as the asynchronous coordinate corresponding to the transition state–plateau–transition state proposed by Dewar[41] and later Tsunda et al.[26] was explored, but no critical points could be found. One is forced to conclude that asymmetric reaction paths documented in previous work[26,41] are artifacts of the constrained reaction coordinate. The only critical point located between benzene and Dewar benzene on the ground state was a totally symmetric transition state, similar to that proposed by Dewar[42] and Tsunda,[26] which was characterized via an analytic second-derivative calculation (Figure 2a). This structure corresponds to the transition state along a symmetric coordinate from benzene to Dewar benzene where the bridgehead bond and the pair of "quinoid" double bonds of Dewar benzene are being synchronously created.

The ground-state potential energy surface in the region linking benzene and benzvalene has been found to have a much more

(39) Newton, M. D.; Schulman, J. M.; Manus, M. M. *J. Am. Chem. Soc.* **1974**, *96*, 17–23.
(40) Liu, R.; Zhou, X.; Pulay, P. *J. Phys. Chem.* **1992**, *96*, 3669–3674.
(41) Dewar, M. J. S.; Kirschner, S.; Kollmar, H. W. *J. Am. Chem. Soc.* **1974**, *96*, 7579–7581.
(42) Dewar, M. J. S.; Ford, G.; Rzepa, H. S. *J. Chem. Soc., Chem. Commun.* **1977**, 728–730.

interesting and surprising topology. There are several minima and transition states separated by a few kilocalories per mole. We begin with prefulvene (6), which is shown in Figure 2b. This structure has long been proposed as an intermediate on the path to benzvalene and fulvene. It has a quasidiradical nature with one radical center located at the pinnacle of the cyclopropanyl moiety and another delocalized over the allylic fragment. The molecule has C_s symmetry and, on the basis of our calculations, is a transition state with a very small imaginary frequency (146i cm^{-1}), which contradicts previous studies in which prefulvene has been characterized as a minimum.[18,19] The reaction path (IRC) from prefulvene leads to a minimum (Figure 2d) structure, which we shall call prebenzvalene, in which the prefulvene structure has distorted toward one of two possible benzvalenes. (The existence of the prebenzvalene region was suggested in early MINDO/3 computations.[43] This structure has almost the same energy (0.2 kcal mol^{-1} lower) as the prefulvene structure, reflecting the extremely flat nature of this region of the potential energy surface.

Two transitions states, within approximately 1 kcal mol^{-1}, were located along a reaction path leading from prebenzvalene (Figure 2d) back to benzene (Figure 2c) and forward (Figure 2e) toward benzvalene. The first of these (Figure 2c) is essentially the transition state for the breaking of the "prefulvene σ-bond" on the asymmetric reaction path from prebenzvalene to benzene. The second structure (Figure 2e) on the reaction path from prebenzvalene to benzvalene is the transition structure for the synchronous formation of the new σ-bond (the 1–5 bond in Figure 2e is 2.29 Å) and the π-bond (the 3–4 bond in Figure 2e is 1.38 Å) in the "cyclopentenyl" ring required for ring closure to benzvalene.

To summarize, it appears that in the region of the "classical" prefulvene structure there is a family of distorted structures we term "prebenzvalenes" which span what is essentially a high-energy plateau region. We have characterized transition states on the backward reaction path to benzene and on the forward reaction path to benzvalene. The prefulvene structure is a transition state linking the two possible prebenzvalene minima. It could be argued that the precise nature of the potential energy surface in the prebenzvalene region of the surface will depend on the nature of the basis set used and inclusion of dynamic correlation. In recent work,[44] we have examined this question for the similar flat biradicaloid intermediate region of the potential surface that occurs for the cycloaddition of two ethylene molecules. While the energetic data change slightly with the use of a better basis and the inclusion of dynamic correlation, the detailed topology of the surface is correctly reproduced at the MC-SCF/4-31G level.

B. Excited-State Potential Energy Surfaces. I. Photochemical Reaction Coordinate Originating in S_1 Benzene. From S_1 benzene the sole product of the nonadiabatic valence isomerization reaction is benzvalene in the liquid phase. (Fulvene, an isomer of benzene, is assumed to be formed via secondary isomerization of the benzvalene produced.) Thus, in order to document a mechanism for this reaction we must locate minima and transition states on S_1 as well as the Born–Oppenheimer violation region.

The only minimum found on this potential surface has symmetry D_{6h} (Figure 3a). One may think of this covalent state as the "anti-Kekule" valence bond isomer. The π-bonds have lengthened to 1.43 Å from the ground-state value of 1.39 Å. Along a coordinate on the excited state from this minimum toward the ground-state prefulvene structure, a transition state was located (Figure 3b) 23 kcal mol^{-1} above the minimum. This structure has a geometry in qualitative agreement with that determined by Kato[19] using an approximate coordinate driving approach and an STO-3G basis. An IRC calculation was performed from this transition state. In the reverse direction it terminates in the D_{6h} minimum (Figure 3a), and in the forward direction it terminates in the Born–Oppenheimer violation region at a prefulvene-like

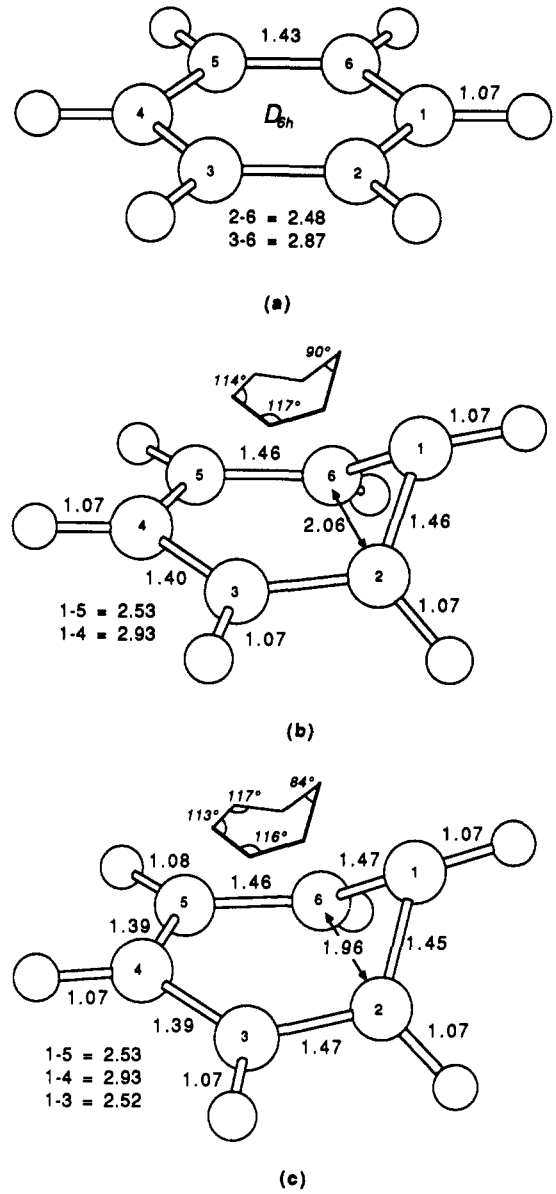

Figure 3. Optimized geometries on S_1 (a) anti-Kekule minimum, (b) anti-Kekule minimum → prefulvene transition state, and (c) prefulvene-like conical intersection.

geometry in which the excited state and the ground state are degenerate.

This prefulvene-like region of the S_1 surface where the IRC terminated was then confirmed as a conical intersection (i.e., the minimum energy point of the $(n-2)$-dimensional crossing surface where the S_0 and S_1 surfaces are degenerate has been fully characterized using the constrained optimization discussed previously). The optimized geometry of the lowest energy point on the intersection is shown in Figure 3c and differs from that of prefulvene primarily in the closing cyclopropanyl σ-bond length.

From a practical point of view, when we optimize the geometry of a conical intersection point, we end up at an arbitrary point in the immediate vicinity of the apex of the cone. Thus, in general, it is incorrect to attribute any significance to gradient difference vector $\mathbf{x}_1$ and nonadiabatic coupling vector $\mathbf{x}_2$ independently; only the plane spanned by these vectors ($\mathbf{x}_1\mathbf{x}_2$) has any meaning. On the other hand, a particular reaction path on the excited surface will undoubtedly have a direction which points at the apex of the cone. In this case, $\mathbf{x}_2$, the nonadiabatic coupling vector, takes on a physical significance in its own right. In dynamics studies (see, for example, reference 45), *the effective direction for the surface*

(43) Dewar, M. J. S.; Kirschner, S. *J. Am. Chem. Soc.* **1975**, *97*, 2932–2933.

(44) Bernardi, F.; Bottoni, A.; Olivucci, M.; Robb, M. A.; Venturini, A. *Chem. Phys. Lett.* **1992**, 229–235.

(45) Blais, N. C.; Truhlar, D. G.; Mead, C. A. *J. Chem. Phys.* **1988**, *89*, 6204.

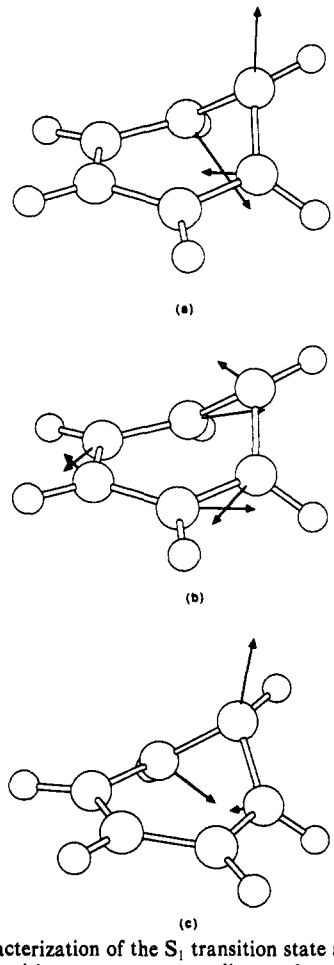

Figure 4. Characterization of the S_1 transition state and conical intersection. (a) Transition vector corresponding to the reaction path anti-Kekule minimum → prefulvene. (b) Nonadiabatic coupling vector evaluated at a geometry on the reaction path near the conical intersection. (c) Gradient difference vector.

hop is taken to be parallel to the direction of the nonadiabatic coupling matrix element $\mathbf{x}_2$. In a dynamics computation, the system will decay when the gap becomes sufficiently small (i.e., at a point near the conical intersection). When a surface hop occurs, in order to conserve total energy, one must adjust one component of the momentum in the "direction" of the nonadiabatic coupling vector. Thus the direction of the original momentum along the excited-state trajectory (i.e., directed toward the apex of the cone, $\mathbf{x}_1$) will be diverted by the effect of the derivative coupling $\mathbf{x}_2$ during the surface hop.

We have computed the nonadiabatic coupling and gradient difference vectors in the region of the minimum of the conical intersection during the optimization process. However, in view of the discussion of the preceding paragraph, since we have a well-defined reaction path that leads from a transition state on S_1 into the conical intersection, it is more instructive to give the vectors $\mathbf{x}_1$ and $\mathbf{x}_2$ at a point on the reaction path itself in the immediate vicinity of the conical intersection. The results are shown in Figure 4a–c. In Figure 4a we show the normal coordinate with the imaginary frequency at the transition structure of Figure 3b, while in Figures 4b and 4c we show the nonadiabatic coupling vector $\mathbf{x}_2$ and the gradient difference vector $\mathbf{x}_1$, respectively, at a point on the IRC near the conical intersection. These two vectors define the two-dimensional geometric subspace in which the degeneracy is lifted at the conical intersection itself, and the nature of this subspace at the minimum energy point of the conical intersection is essentially the same, although $\mathbf{x}_1$ and $\mathbf{x}_2$ may be rotated among themselves.

In Figures 4b and 4c we see that the space of $\mathbf{x}_1$ and $\mathbf{x}_2$ corresponds to a subspace of nuclear motion that corresponds to (i) an interconversion between two localized Kekule VB structures (Figure 4b, the nonadiabatic coupling vector) and (ii) a benzene-to-prefulvene interconversion coordinate (Figure 4c, gradient difference vector). As we have just discussed, when the system emerges from the minimum of the Born–Oppenheimer violation region onto the ground-state surface, the ground-state reaction path will lie in the plane $\mathbf{x}_1\mathbf{x}_2$. As expected, the gradient difference vector $\mathbf{x}_1$ (Figure 4c) is essentially parallel to the reaction coordinate (Figure 4a) corresponding to motion toward the apex of the cone along the benzene-to-prefulvene interconversion coordinate leading to products. However, if the system decays before the apex of the cone, there will be some acceleration in the direction of the nonadiabatic coupling vector $\mathbf{x}_2$ which corresponds to the interconversion coordinate between two localized Kekule structures. Motion in this coordinate leads to a high-energy out-of-plane distorted Kekule valence bond structure and then to benzene itself. The possible population of this latter path coupled with the fact that the high-energy prefulvene region of the surface is rather flat (i.e., the barrier between prebenzvalene, Figure 2d, and benzene is 1.3 kcal mol^{-1}) may explain the rather low quantum yield of the reaction. The nature of the conical intersection region, as described by the vectors $\mathbf{x}_1\mathbf{x}_2$, is consistent with the VB description of the states which intersect, namely (i) a combination of Kekule structures and (ii) a prefulvene VB structure. The degeneracy is lifted if one moves along directions that lead to geometries associated with a localized VB structure, e.g., Kekule-like or prefulvene-like.

To conclude this discussion we must emphasize the fact that the crossing surface (i.e., the conical intersection) has dimension $n - 2$. We have characterized only the lowest energy point on this conical intersection in detail. The geometry can be changed in all directions orthogonal to $\mathbf{x}_1$ and $\mathbf{x}_2$ without lifting the degeneracy (but obviously the energy increases). This fact has implications of the S_2 photochemistry that we will presently document and discuss. However, the fact that the S_0 surface in the prefulvene region of the surface is rather flat implies that any attempt to model the dynamics of the nonradiative decay process using 1- or 2-dimensional models involves rather drastic assumptions.

II. Photochemical Reaction Coordinate for S_2 (D $^1E_{2g}$) Benzene. The S_2 surface for benzene has never been characterized in detail before. The only theoretical result is that of Meisl and Janoschek,[24] who have located a diradicaloid minimum on the surface that correlates with the D $^1E_{2g}$ state of benzene. Their CI result places S_2 (from the D $^1E_{2g}$) below the state that correlates with B $^1B_{1u}$. The $^1B_{1u}$ state of benzene is ionic in character, and therefore a true description is outside the range of validity of our calculations. However, as demonstrated by Roos et al.,[23] the covalent D $^1E_{2g}$ is well described with relatively crude basis sets. In any case, these photochemical reactions involve bond isomerization, so it seems unlikely that ionic and Rydberg states will be important in these processes. Thus we have assumed that benzene initially excited into the $^1B_{1u}$ state has rapidly crossed to the covalent state originating from $^1E_{2g}$ before the chemical reaction takes place in the region of the diradicaloid minimum.

Since the vertically excited covalent D $^1E_{2g}$ state is essentially a combination of the Dewar VB resonance forms, we expect that this surface will have a low-energy region characterized by structures that are essentially quinoid in nature with two short C_2–C_3 and C_5–C_6 bonds and a pair of biradical centers C_1 and C_4. The lowest energy planar quinoid structure is shown in Figure 5a and has D_{2h} symmetry. A second-derivative calculation showed this structure to be a third-order saddle point (i.e., three imaginary frequencies). The lowest energy regions of the S_2 surface are associated with "boat" structures, and the only minimum we have been able to characterize is shown in Figure 5b. A flattened "chair" structure was also optimized and is shown in Figure 5c. Remarkably, this structure is a transition structure ($72i$ cm^{-1}) that connects two equivalent "half-boat" structures along the negative direction of curvature. The "half-boat" structure itself (shown in Figure 5d) corresponds to the Born–Oppenheimer violation region where S_1 and S_2 are degenerate. This structure has been fully optimized and characterized as the lowest energy point on

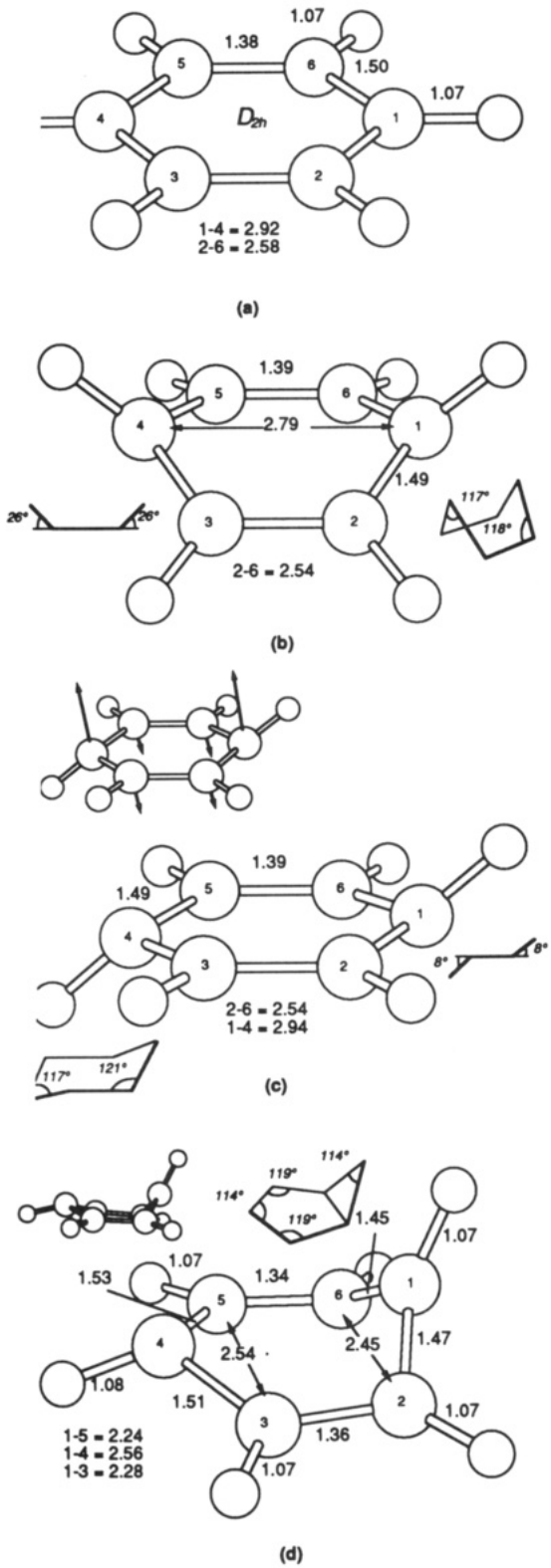

Figure 5. Optimized geometries on the S_2 (a) planar quinoid structure (three imaginary frequencies), (b) quinoid biradical minimum, (c) half-chair transition state, and (d) lowest energy point on the S_2/S_1 conical intersection.

the S_1/S_2 conical intersection, as we will now discuss.

The nature of the S_1/S_2 conical intersection can be understood from the directions of the nonadiabatic coupling and gradient difference vectors computed in the region of the minimum of the conical intersection shown in Figures 6a and 6b, respectively. The plane of the two vectors $\mathbf{x}_1$ and $\mathbf{x}_2$ that lift the degeneracy of the $(n-2)$-dimensional crossing surface corresponds to a quinoid-to-antiquinoid motion, which changes the C_2–C_3 and C_5–C_6 distances, combined with a 1,3 and 1,4 bond formation. Clearly,

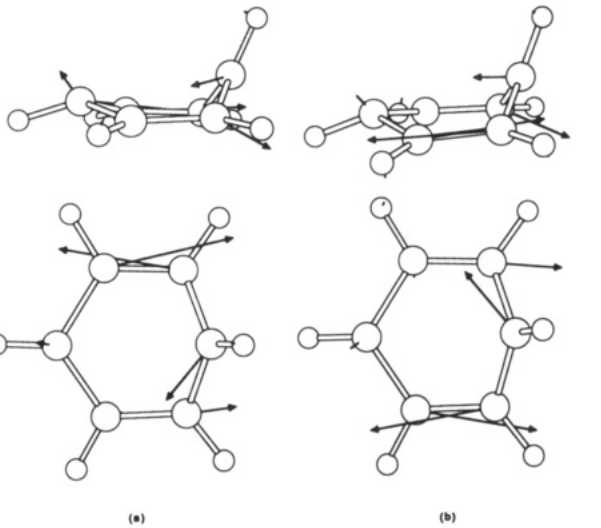

Figure 6. Characterization of the lowest energy point on the S_2/S_1 conical intersection. (a) Nonadiabatic coupling vector. (b) Gradient difference vector.

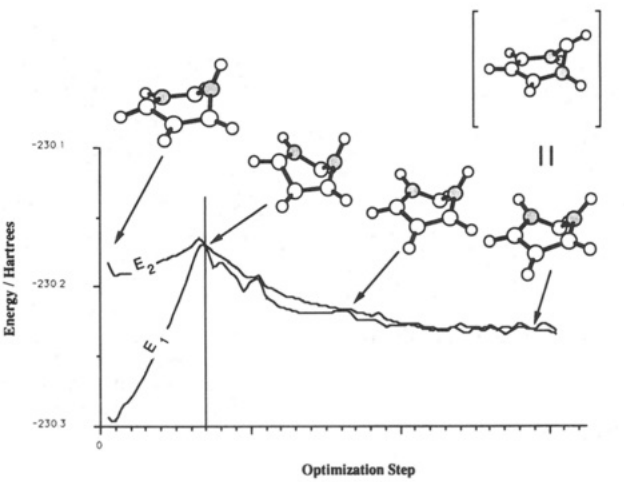

Figure 7. Search for the S_1/S_0 crossing surface in the vicinity of the lowest energy point on the S_2/S_1 conical intersection. Up to the vertical bar we are searching for a point on the S_1/S_0 crossing surface. After the vertical bar we converge to the S_1/S_0 crossing surface minimum.

motion in this plane encompasses reaction paths to both prefulvene and Dewar benzene.

The existence of a low-energy diradicaloid minimum on S_2 with an immediately adjacent S_1/S_2 Born–Oppenheimer violation region at only slightly higher energy suggests that the radiationless decay from S_2 is almost completely efficient in contrast to the commonly held view. Why, then, does one apparently see a photochemistry distinct from that of S_2? The answer lies in the relation between the S_0/S_1 and the S_1/S_2 Born–Oppenheimer violation regions and the fact that the S_1/S_0 crossing surface can actually extend into the immediate vicinity of the S_2/S_1 conical intersection.

In order to observe a different photochemistry from S_2, the system should decay almost immediately from S_1 after the S_1/S_2 crossing. Thus the S_0/S_1 decay that follows after the S_1/S_2 decay must occur at a geometry on the S_0/S_1 crossing surface that is different from (at a higher energy than) the S_0/S_1 (prefulvene-like) crossing minimum. We can provide a model for understanding this effect by searching for *the point on the S_0/S_1 surface crossing that is immediately adjacent to the lowest energy point on the S_1/S_2 conical intersection.* Obviously, this point is not the minimum of the S_0/S_1 crossing surface; however, it is likely that the reaction path from S_2 will enter the S_0/S_1 crossing surface at the energy of the S_1/S_2 conical intersection. In Figure 7 we illustrate the energy and geometries that correspond to (a) searching for a point on the S_0/S_1 crossing surface that is immediately adjacent

Scheme II

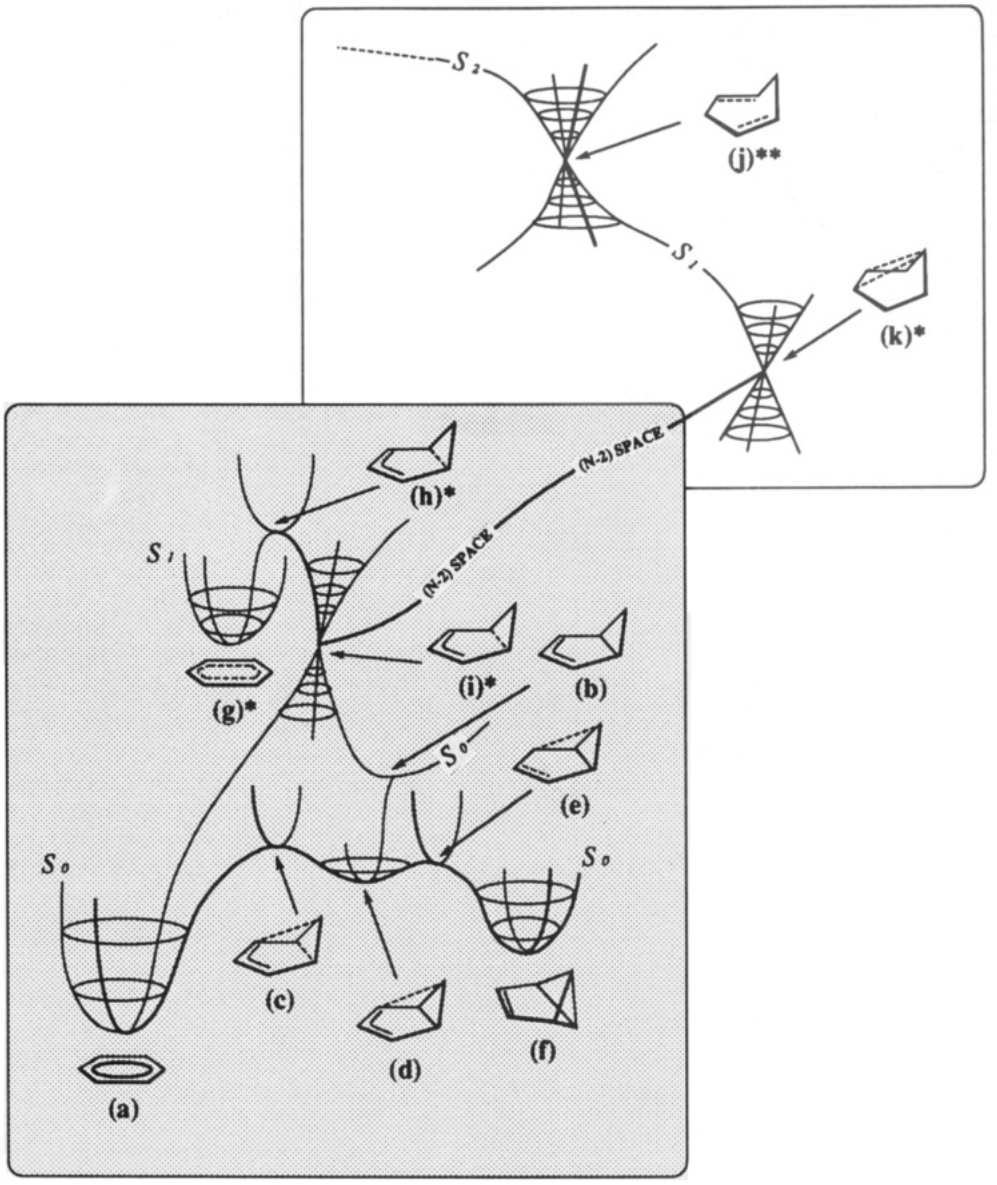

to the minimum of the S_1/S_2 crossing, and (b) following this S_0/S_1 crossing surface down to the minimum. The geometry of the point on the S_0/S_1 crossing surface that is immediately adjacent to the minimum of the S_1/S_2 crossing is illustrated in Figure 8. The energy of this point is only 5 kcal mol^{-1} higher (Table I) than the S_1/S_2 crossing surface minimum. The most important features of this geometry are that (a) there is a C_1–C_4 bond that is slightly longer (2.47 Å) than the bridgehead bond in the S_0 transition state between Dewar benzene and benzene (2.24 Å) and (b) there is a C_1–C_3 bond that is almost the same as the C_1–C_3 at the S_0/S_1 crossing surface minimum. Thus from this S_0/S_1 crossing region that is adjacent to the S_1/S_2 crossing minimum one can reach either benzvalene or Dewar benzene.

Conclusions

The interrelationship between the S_0, S_1, and S_2 reaction paths is illustrated in Scheme II. It must be emphasized that this is only a schematic representation of the surfaces of ground and excited states and is merely designed to convey the nature of critical points and their approximate relationship. Nevertheless, this representation is useful for documenting the mechanistic scenario for benzene photochemistry that is suggested by our results.

The S_1 photochemistry of benzene yields benzvalene **f**.[7-10] The excited-state reaction path has been characterized by an excited-state minimum with D_{6h} symmetry **g***, and a transition state

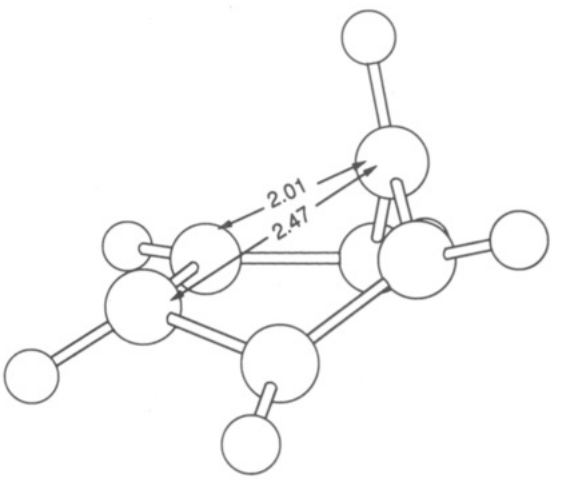

Figure 8. Geometry of the S_1/S_0 crossing surface in the vicinity of the lowest energy point on the S_2/S_1 conical intersection (i.e., at the vertical bar in Figure 7).

h* between this minimum and a prefulvene biradicaloid **b** that occurs on the ground-state surface. The Born–Oppenheimer violation region has been characterized by optimizing the lowest energy point on the conical intersection **i***.

The computed S_1 reaction path involves passage over the transition state **h*** followed by return to the ground state via a fully efficient decay through the conical intersection region **i*** near prebenzvalene **d**. This reaction path is consistent with a channel 3 decay mechanism (loss of fluorescence[8,11-13] above the critical threshold of 3000 cm^{-1} or 8.6 kcal mol^{-1}) that corresponds to photochemical conversion of the excited molecule to the isomeric benzvalene and also with the photochemical observation[2] that the quantum yield of benzvalene is wavelength dependent. (Dynamics calculations indicate that decay through a conical intersection occurs within one vibrational period[37].) The computed nonadiabatic coupling and gradient difference vectors give some rationalization of the experimental observation that the disappearance of observed fluorescence is not accompanied[2] by a significant rise in the (small) quantum yield of benzvalene. While one of the two vectors that lift the degeneracy corresponds to motion along the benzene-to-prefulvene interconversion coordinate, the other corresponds to motion along the interconversion coordinate between two localized Kekule structures and leads to a high-energy out-of-plane distorted Kekule valence bond structure and back to benzene itself. Further, the flat nature of the ground-state surface in the prefulvene region **b-c-d-e** implies that topological control of the reaction is lost. There is almost no barrier on a reaction from the prebenzvalene intermediate **d** back to benzene itself.

The surprising aspect of benzene photochemistry is related to S_2. Our results show that the different photochemistry attributed to S_2 is, in fact, not due to S_2 directly at all, since the crossing to S_1 is fully efficient via the conical intersection **j**** of S_2/S_1. Rather, the occurrence of Dewar benzene as a product of S_2 photochemistry is due to the fact that the S_0/S_1 crossing surface will be entered at the region **k***, well above the minimum **i*** of the S_0/S_1 crossing surface, with a geometry that can be a precursor of either Dewar benzene or benzvalene. In other words, **k*** and **i*** lie on the same $(n-2)$-dimensional S_0/S_1 crossing surface. This result is consistent with experimental observations[20] that both benzvalene and Dewar benzene may be produced via selective population of S_2 and S_3. With initial energies sufficient only to overcome the barrier on S_1, only benzvalene is produced via the mechanism described above. When there is an excess of energy (decay from higher excited states), the system has access to higher energy points on the S_0/S_1 crossing surface with different geometries, yielding a wider distribution of products subsequent to decay. It must be noted that the molecules returning to the ground state at such points will be extremely "hot" and efficient relaxation channels will be necessary for the system to relax into the high-energy valence isomer minima. Thus, one does not observe Dewar benzene from benzene vapor-phase photolysis.

In this work we have demonstrated that the products of benzene photochemistry appear to be controlled by the topology of the S_0/S_1 crossing surface. While we have only fully optimized the minimum of this crossing surface, we have also been able to demonstrate that this surface is accessible in the region of the S_1/S_2 crossing minimum. Thus, the photochemistry must depend on the energy used in the experiment (and thus dynamical considerations) and the detailed topology of this crossing surface. This conjecture has some experimental support in the fact that in substituted[2,5] or site perturbed benzenes[46] one observes different photoproducts. In hexafluorobenzene, the Dewar benzene isomer is the major product of photolysis from S_2, with fluorescence occurring from S_1. In an argon matrix[46] where benzene is "site perturbed", one observes Dewar benzene via photolysis with a source of 253.7 nm.

Acknowledgment. This research has been supported by the SERC (U.K.) under Grant No. GR/G 03335. Ian Palmer is grateful to the SERC (U.K.) for the award of a studentship. The authors are also grateful to IBM for support under a Joint Study Agreement. All computations were run on an IBM RS/6000.

(46) Johnstone, D. E.; Sodeau, J. R. *J. Phys. Chem.* **1991**, *95*, 165-169.

Electron Donor-Acceptor Complexes as Potential High-Efficiency Second-Order Nonlinear Optical Materials. A Computational Investigation

Santo Di Bella,† Ignazio L. Fragalà,† Mark A. Ratner,* and Tobin J. Marks*

Contribution from the Department of Chemistry and the Materials Research Center, Northwestern University, Evanston, Illinois 60208-3113. *Received March 16, 1992*

Abstract: The second-order nonlinear optical response of model molecular 1:1 and asymmetric 2:1 organic π electron donor-acceptor (EDA) complexes is investigated using the INDO/S sum-over-excited particle-hole-states formalism. It is found that intermolecular charge-transfer transitions in EDA complexes represent a promising approach to achieving sizable second-order optical nonlinearities. Calculated hyperpolarizabilities may be generally related to the strength of the donor-acceptor interaction in the complex, affording for a given acceptor, the largest values in the case of aminoarene donors. The large change in dipole moment that accompanies intermolecular charge-transfer transitions and the relatively low-lying charge-transfer excitation energies are the major sources of the large calculated second-order nonlinearities. The relative orientation of donor and acceptor components is also an important feature, leading to stabilization of the ground state as well as to maximization of the oscillator strength of the lowest energy charge-transfer excitation and, in turn, the NLO response. In the case of asymmetric 2:1 EDA complexes, calculated hyperpolarizability enhancements over the 1:1 complexes can be related to the red-shift of the charge-transfer excitation as well as to an increase in dipole moment change between ground and excited states. The perturbation theoretical "two-level" model is a useful first approximation for predicting the second-order nonlinear response of such complexes.

Introduction

An indispensable prerequisite for achieving large second-order nonlinear optical (NLO) response in molecular chromophores is the existence of strong intramolecular charge-transfer (CT) excitations.[1] This can be understood in terms of perturbation theoretical arguments,[1] which consider the effect of an oscillating

† Permanent address: Dipartimento di Scienze Chimiche, Università di Catania, 95125 Catania, Italy.

(1) (a) Boyd, R. W. *Nonlinear Optics*; Academic Press: New York, 1992. (b) Prasad, P. N.; Williams, D. J. *Introduction to Nonlinear Optical Effects in Molecules and Polymers*; Wiley: New York, 1991. (c) Shen, Y. R. *The Principles of Nonlinear Optics*; Wiley: New York, 1984.

0002-7863/93/1515-682$04.00/0